

# Experimental study of Bernoulli's equation with losses

Martín Eduardo Saleta<sup>a)</sup>

*Escuela de Ciencia y Tecnología de la Universidad Nacional de San Martín—Buenos Aires, Argentina 1653 and Departamento de Física “J. J. Giambiagi”—FCEyN—Universidad de Buenos Aires, Argentina 1428*

Dina Tobia<sup>b)</sup>

*Departamento de Física “J. J. Giambiagi”—FCEyN—Universidad de Buenos Aires, Argentina 1428*

Salvador Gil<sup>c)</sup>

*Escuela de Ciencia y Tecnología de la Universidad Nacional de San Martín—Buenos Aires, Argentina 1653 and Departamento de Física “J. J. Giambiagi”—FCEyN—Universidad de Buenos Aires, Argentina 1428*

(Received 11 August 2004; accepted 17 December 2004)

We present a simple and inexpensive experiment to study the drainage of a cylindrical vessel. The experiment consists of a transparent cylinder and a webcam or a digital camera connected to a computer. The model proposed to explain the results makes use of Bernoulli's equation for real flows including energy losses. The experimental results are well explained by the model, which is a generalization of Torricelli's expression. © 2005 American Association of Physics Teachers.

[DOI: 10.1119/1.1858486]

## I. INTRODUCTION

The Bernoulli equation has application in many branches of science and engineering.<sup>1–3</sup> General forms of Bernoulli's equation that are valid for viscous fluids have been discussed.<sup>4</sup> Nonetheless, there are few experiments accessible to beginning and intermediate students that illustrate the use of Bernoulli's equations for viscous fluids.<sup>5,6</sup>

We present a conceptually simple and inexpensive experiment to study the drainage of a cylindrical vessel. The experiment is essentially a recreation of Torricelli's experiment,<sup>1,2</sup> with the benefit of new technologies. We first present a model based on the Bernoulli equation for real flows. Then we discuss the basic characteristics of the experiment and the experimental results. The experiment lets us thoroughly test the implications of the model and extract the relevant parameter associated with energy losses. The experiment is a useful introduction to the Bernoulli equation for real flows and involves concepts that are relatively simple to discuss. The physics is easy to visualize, and it is straightforward to quantitatively test the implications of the model.

## II. THEORETICAL CONSIDERATIONS

For Newtonian fluids the shear stress is proportional to the velocity gradient. Therefore the velocity of the fluid at the surface of a solid must be zero; otherwise, the velocity gradient and the shear stress would be infinite. Only for an ideal fluid, that is, a fluid with zero viscosity,  $\eta=0$ , is it possible to have a finite velocity at the surface of a solid. When a real fluid flows through the interior of a tube or between two surfaces, there are two effects that are a consequence of a nonzero viscosity. The velocity profile has a maximum at the center of the tube and the mechanical energy in the system is not conserved.

In its simplest form, the Bernoulli equation is a statement of the conservation of mechanical energy per unit of volume along a stream line<sup>1,2</sup>

$$\frac{1}{2}v_1^2 + \frac{P_1}{\rho_1} + gz_1 = \frac{1}{2}v_2^2 + \frac{P_2}{\rho_2} + gz_2. \quad (1)$$

The subscripts 1 and 2 refer to different points in the flow, 1 being upstream of 2,  $v$  is the local velocity of the fluid,  $g$  is the local acceleration of gravity,  $P$  is the pressure, and  $z$  is the vertical height of the point.

In the presence of viscosity, Bernoulli's equation becomes an expression of energy balance, and often is expressed in terms of energy per unit volume or the pressure between two points in the fluid. The Bernoulli equation for a steady flow of a real fluid in a pipe can be written as<sup>1–4</sup>

$$\frac{1}{2}\alpha_1 u_1^2 + \frac{P_1}{\rho_1} + gz_1 = \frac{1}{2}\alpha_2 u_2^2 + \frac{P_2}{\rho_2} + gz_2 + \Delta w_{\text{loss}}. \quad (2)$$

The average velocity,  $u$ , of the flow along the tube is defined in terms of the flux  $Q$  as

$$Q = \int \int_S \mathbf{v} \cdot d\mathbf{S} = \mathbf{u} \cdot \mathbf{S}, \quad (3)$$

where  $\mathbf{S}$  is the area of the normal cross section of the flow (or pipe) and  $\mathbf{v}$  is the local velocity. Equation (3) can be regarded as the definition of the average velocity  $\mathbf{u}$ . An important physical consequence of the presence of shear stress against the walls of the tube is that the velocity profile of the flow across the tube is no longer constant. The kinetic energy coefficients  $\alpha_i$  in Eq. (2) represent the ratio between the actual kinetic energy that flows through a normal cross section and the kinetic energy of the same flux, but with the uniform velocity profile equal to  $u$ . More specifically,  $\alpha$  is defined as<sup>1,3</sup>

$$\alpha = \int \int_S v^2 \mathbf{v} \cdot d\mathbf{S} / u^3 S. \quad (4)$$

Thus, the term  $\alpha u^2/2$  in Eq. (2) represents the kinetic energy flow per unit of mass across a surface normal to the pipe. For a uniform profile  $\alpha=1$ ; for a nonuniform profile, it follows straightforwardly from Eqs. (3) and (4) that  $\alpha>1$ ; for a parabolic profile of velocity (laminar flow)  $\alpha=2$ .

For real fluids, mechanical energy is dissipated in the viscous boundary layer along the pipe walls and changes in the velocity profiles in entries and exits (minor losses). The term

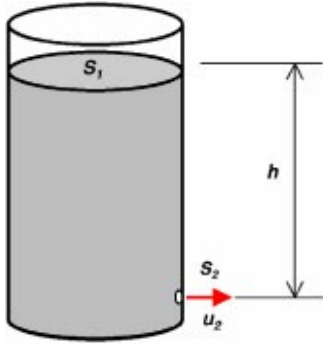


Fig. 1. Schematic diagram of the vessel.

$\Delta w_{\text{loss}}$  in Eq. (2) represents these energy losses between points 1 and 2. Usually the presence of restrictions in the flow leads to the formation of turbulence, which is the main source of energy losses. There is no general expression for these types of losses. Nonetheless, different expressions that describe these energy losses can be obtained from dimensional analysis for particular cases.<sup>1,2</sup> The relevant constants associated with these expressions need to be determined from experimental studies. Also experiments indicate that whenever there is a restriction in the flow produced by bends, tees, valves, and the like, a drop in pressure appears across the component. This pressure drop depends on the geometry of the restriction and has been observed to be proportional to the flow rate squared,<sup>1,2</sup> that is,  $\Delta P \propto Q^2 \propto u^2$ .

As we have mentioned, the presence of obstructions in the flow usually leads to the formation of turbulent wakes. These changes in the flow pattern produce large transfers of momentum from the originally regular flow to the eddy currents and also are associated with a significant increase in the entropy of the system. This entropy increase,  $\Delta S$ , requires the additional removal of mechanical energy from the flow,  $\Delta q = T\Delta S$ . Because the complexity of turbulence is far beyond the scope of the present study, we refer the reader to a review of the literature on turbulence.<sup>7</sup>

We will make the ansatz that  $\Delta w_{\text{loss}}$  can be expressed as the sum of two terms, one depending on the square of the average velocity and the other independent of the velocity, and let the experiment test our ansatz.

If we apply Bernoulli's equation including losses to our system and take into account that the pressure at the free surface and at the exit orifices is the atmospheric pressure  $P_0$ , from Eq. (2) (see Fig. 1), we have

$$\frac{1}{2g}u_2^2 + \frac{1}{2g}ku_2^2 + \Delta Z = h + \frac{\alpha_1}{2g}u_1^2. \quad (5)$$

The second term on the left-hand side of Eq. (5) represents the energy loss term, where the constant  $k$  is the coefficient of minor losses at the exit orifice located at point 2.<sup>1,2</sup> The quantity  $\Delta Z$  represents the part of the energy loss that is independent of the velocity. As justified in the Appendix, the velocity coefficient  $\alpha_2 = 1$  for the exit jet through the orifice. The variable  $h (= z_1 - z_2)$  represents the height of the free surface relative to the position of the exit orifice.

The velocities  $u_1$  and  $u_2$  are related by the continuity equation (conservation of mass). For an incompressible fluid, ( $\rho_1 = \rho_2$ ) we have

$$d_2^2 C_v u_2 = d_1^2 u_1. \quad (6)$$

Here  $d_1$  and  $d_2$  represent the diameters of the vessel and the orifice, respectively.  $C_v$  is the coefficient of vena contracta,<sup>1-3</sup> which is related to the fact that the cross section of the exit jet is smaller in general than that of the exit orifice. By combining Eqs. (5) and (6), we obtain

$$u_2^2 = \frac{2g(h - \Delta Z)}{\left[1 + k - \alpha_1 \left(\frac{d_2}{d_1}\right)^4 C_v^2\right]}. \quad (7)$$

Because  $d_1$  is considerably larger than  $d_2$  ( $d_2/d_1 \approx 0.03$ ) in our case and  $C_v < 1$ , Eq. (7) can be simplified to

$$u_2^2 \cong \frac{2g}{[1 + k]}(h - \Delta Z). \quad (8)$$

Thus, if we can measure the velocity of the exit jet  $u_2$  as a function of  $h$ , we expect a linear relation between  $u_2^2$  and  $h$ . This linear trend could be used to experimentally test our model. Furthermore, the slope of this line and its intersection with the axis would allow us to determine experimentally the values of the coefficients  $k$  and  $\Delta Z$ .

From this model, it is possible to determine the motion of the free surface  $u_1$  and the evacuation or empty time  $t_e$ ,<sup>6</sup> which is the time it takes the vessel to empty from a height  $h_0$ . We combine Eqs. (6) and (8) and find

$$u_1 = -\frac{dh}{dt} = -C_v \left(\frac{d_2}{d_1}\right)^2 \sqrt{2g\mu} \sqrt{h - \Delta Z}, \quad (9)$$

where we have introduced the coefficient  $\mu = 1/(1 + k)$ . The sign in Eq. (9) is related to the orientation chosen to define the positive direction of  $h$  and  $u_1$ . We introduce the constant  $A_0$  as

$$A_0 = C_v \left(\frac{d_2}{d_1}\right)^2 \sqrt{2g\mu} \quad (10)$$

and write a differential equation for  $h$

$$\frac{dh}{\sqrt{h - \Delta Z}} = -A_0 dt. \quad (11)$$

Equation (11) can be easily integrated to give

$$\frac{\sqrt{h - \Delta Z}}{\sqrt{h_0 - \Delta Z}} = \left(1 - \frac{t}{t_e}\right), \quad (12)$$

where  $h_0$  is the height of the free surface at  $t = 0$  and  $t_e$  is the empty time, which according to Eqs. (10) and (12), is given by

$$t_e = \frac{\sqrt{h_0 - \Delta Z}}{C_v \left(\frac{d_2}{d_1}\right)^2 \sqrt{2g\mu}}. \quad (13)$$

Therefore, if we measure  $h$  as a function of time, a plot of  $\sqrt{h - \Delta Z}$  as a function of  $t$  should be linear. The parameters of this straight line would provide the value of  $t_e$  and allow us to find the value of  $C_v$ . For  $t \approx t_e$ , there is still some fluid above the orifice ( $h \approx \Delta Z$ ), but there is no jet, and the liquid just leaks out of the tank.

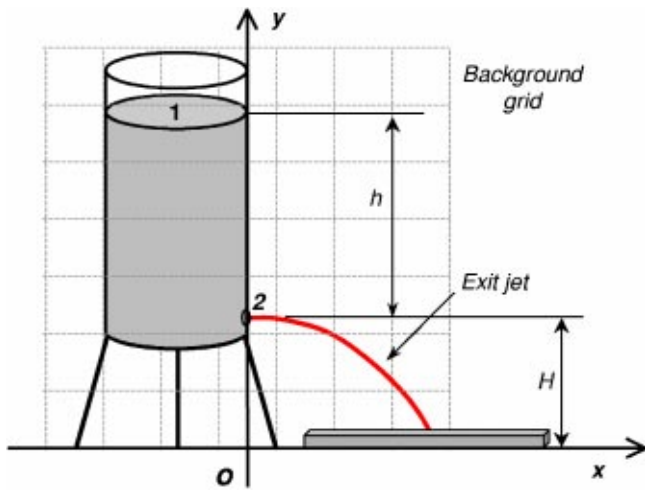


Fig. 2. Schematic diagram of the experimental setup.

To determine the value of  $u_2$ , we shall assume that the motion of the water particles that comprise the jet follow the same equation of motion as those of a horizontal projectile with initial velocity  $u_2$

$$x(t) = u_2 t, \quad (14a)$$

$$y(t) = H - \frac{1}{2} g t^2, \quad (14b)$$

where  $H$  is the height of the exit orifice relative to the origin as shown in Fig. 2. If we combine Eqs. (14a) and (14b), we obtain the equation for the trajectory of the jet

$$y(x) = H - \frac{1}{u_2^2} \left( \frac{g}{2} x^2 \right). \quad (15)$$

Therefore, if we can fit the experimental data of the trajectory of the exit jet of water to Eq. (15), we could obtain the value of  $u_2$ .

### III. EXPERIMENT

The experimental setup consists of a transparent cylindrical tank with a lateral drainage orifice close to the bottom and a webcam connected to a computer. The vessel is 11 cm in diameter and 25 cm high, the diameter of the orifice is 3 mm, and the wall thickness of the vessel is 2 mm. This type of vessel, with a horizontal capillary tube, has been used to determine the viscosity of a fluid.<sup>8</sup> The tank was filled with tap water with a few drops of blue ink to facilitate the visualization of the exit jet. The vessel was positioned in front of a board on which we had drawn a grid with lines every 10 cm to provide an absolute scale for the photographs. The exit jet was parallel to the gridded board. The webcam is placed just in front of the vessel, at about 1.5 m. In this manner we are able to photograph the jet of water with the grid in the background. Pictures were taken every time the free surface dropped by about 1 cm. A digital camera also could be used for this purpose. In this manner, each photograph recorded  $h$ , the height of the water in the cylinder, and the trajectory of the exit jet of water from the orifice. To determine the trajectory of the jet, it is possible to use a graphics program that allows us to obtain the location (pixel coordinate) of any point in the picture. By using the background grid, it is pos-

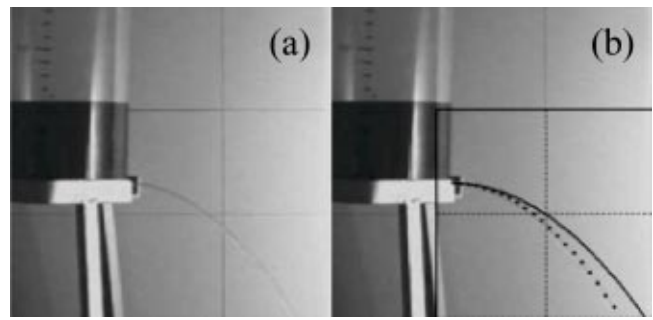


Fig. 3. (a) Digital photograph of the exit jet. (b) The same photograph in the background overlapped with a plot of the theoretical trajectory (dotted line) of the jet as described by Eq. (15). The solid line represents the theoretical expectation if energy loss is completely ignored, as predicted by Eq. (1).

sible to transform the coordinate of any pixel in the photo to the grid coordinate. An alternative is to use the picture as the background of a plot.

The procedure we followed to obtain  $u_2$  from the experimental data is to overlap the digital photograph of the jet with a graph with a transparent background.<sup>9</sup> The grid of the graph is set to coincide with the mesh used in the background of the picture. The graph is moved and stretched so that the mesh of the picture coincides with the corresponding grid in the graph.<sup>9</sup> Once this condition is achieved, the origin (vertex) of the parabola described by Eq. (15) is chosen to coincide with the exit orifice. Then the value of  $u_2$  is varied so that the curve described by Eq. (15) coincides with the experimentally observed trajectory. Figure 3 illustrates this procedure.

To facilitate the measurement of the height  $h$  of the liquid as a function of time, we drew horizontal marks every 0.5 cm, starting at the position of the drainage orifice. We used a stopwatch to measure the time it took for the free surface of the water to reach each horizontal mark.

### IV. RESULTS AND DISCUSSION

A digital photograph of the vessel and the exit jet is shown in Fig. 3(a). In Fig. 3(b) we show the same digital photograph of the exit jet in the background overlapped with a plot of the theoretical trajectory of the jet as given by Eq. (15). By adjusting the value of  $u_2$ , we fitted the theoretical trajectory to the actual path of the jet. Figure 3(b) shows that the trajectory of the jet is well reproduced by Eq. (15). This agreement is a clear indication that the liquid particles that form the jet follow the same trajectory as do solid particles.<sup>10</sup> Therefore the liquid elements of volume are described by the same physical laws of mechanics that govern the motion of solids. This result may be useful for confronting the Aristotelian misconception held by some students that liquid and solids follow different laws. In Fig. 3 we also have included the trajectory of the jet that we would expect if there were no energy loss, Eq. (1); it is clear that the naive application of Eq. (1) gives a poor description of the data.

In Fig. 4, we plot  $u_2^2$  as a function of  $h$ . Because this plot is linear, the main assumptions of our model, expressed by Eqs. (7) and (8), are in good agreement with the experimental results. Furthermore, we can obtain the values of the parameters  $\Delta Z$  and  $k$  by fitting the theoretical expectation, Eq. (8), to the data. In Table I we summarize the values of these parameters for different experimental runs. In Fig. 4 we also

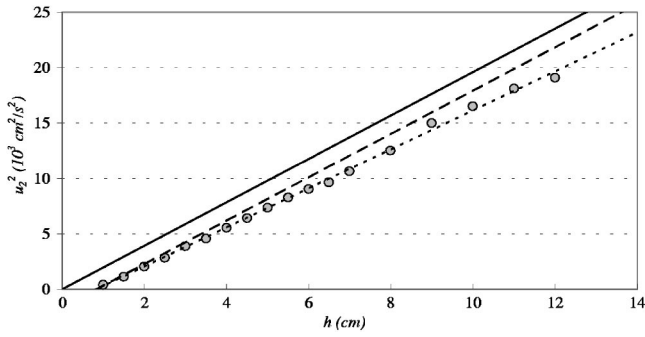


Fig. 4. The circles represent the experimental results of  $u_2^2$  as a function of the height  $h$ ; the dotted line is a linear fit of the data using Eq. (8). The solid line represents Eq. (1). The dashed line is the expectation obtained by ignoring the minor loss term ( $k=0$ ).

show the theoretical expectation that is obtained using Eq. (1). Again we see that this approach gives a poor description of the results. In Fig. 4 we also include the line that would be obtained from Eq. (8) if we ignored the minor loss term ( $k=0$ ); again the agreement of this approximation with the data is poor. Therefore the results of the experiment indicate that it is necessary to include two types of energy losses in Bernoulli's equation, one dependent on the square of the average velocity (minor loss) and the other independent of the velocity ( $\Delta Z$ ).

In Fig. 5 we present the results for the height  $h$  of the free surface as a function of time. To test the validity of our model, Eq. (12), we plotted the modified variable  $\sqrt{(h-\Delta Z)/(h_0-\Delta Z)}$  as a function of time. The clear linear trend of this plot indicates the validity of our model. In Fig. 5 we also include the theoretical expectation that we would obtain if we ignore the effect of vena contracta, that is,  $C_v=1$ . We see that our results are inconsistent with this assumption and indicate the necessity of taking into consideration the contraction of the jet. The parameters of the fitted line allow us to obtain the values of the empty time  $t_e$  and  $C_v$ . From Table I we see that the values of the parameters are consistent for the different runs. The value of  $k$  and  $C_v$  are consistent with the values reported in the literature.<sup>1-3</sup>

There is a simple heuristic justification for the contraction of the jet.<sup>2,11</sup> The momentum of the discharge jet is along the horizontal axis (the  $x$  axis in Fig. 2); the rate of change of the momentum is  $dp/dt = \rho Q u_2$ . Here  $Q$  is the volume flow rate ( $Q = C_v A u_2$ ) and  $A$  represents the outlet area. The force responsible for this change of momentum is associated with the hydrostatic pressure,  $P = \rho g h$ , that is

$$PA = \rho g h A \approx C_v A \rho u_2^2. \quad (16)$$

Therefore, according to Eq. (8) we have

Table I. Parameters obtained for several runs. The values of  $\mu$  and  $C_v$  are consistent with those reported in the literature (see Refs. 1-3).

Parameter	Run 1	Run 2	Run 3
$\Delta Z$ (cm)	$0.9 \pm 0.2$	$0.9 \pm 0.2$	$0.9 \pm 0.2$
$\mu$	$0.91 \pm 0.01$	$0.90 \pm 0.01$	$0.90 \pm 0.01$
$k$	$0.09 \pm 0.01$	$0.11 \pm 0.01$	$0.11 \pm 0.01$
$C_v$	$0.46 \pm 0.03$	$0.47 \pm 0.03$	$0.44 \pm 0.03$

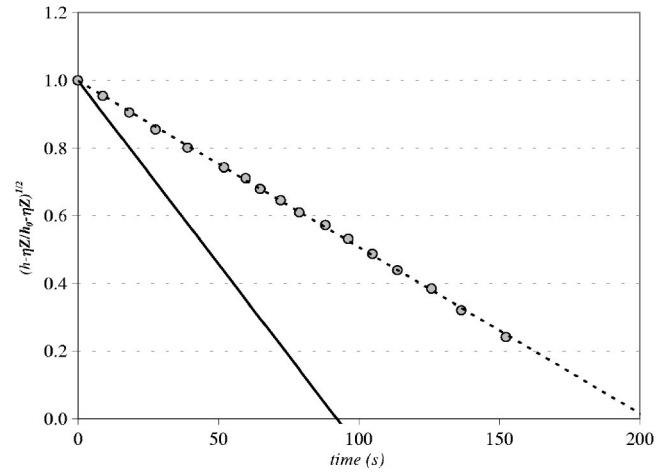


Fig. 5. The circles represent the experimental results of  $\sqrt{(h-\Delta Z)/(h_0-\Delta Z)}$  as a function of time; the dotted line is a fit of the data. The solid line represents the theoretical expectation obtained disregarding the contraction of the jet ( $C_v=1$ ).

$$C_v \approx \frac{1}{2} \left( \frac{1+k}{1-\Delta z/h} \right) \approx 0.59 < 1. \quad (17)$$

This simple argument provides us with a physical justification for the contraction of the jet and also gives a semiquantitative estimate of  $C_v$ . Note that the contraction of the jet is also a consequence of the complex instabilities that take place around the orifice. The observed values of  $C_v$  depend, among other things, on the roundness of the edges of the aperture and the wall thickness.<sup>1</sup> These effects are not accounted for by our simplified argument.

At low velocities the fluid travels smoothly in regular paths or streamlines. This flow pattern is referred to as laminar or streamline flow. As the velocity increases, the fluid flow begins to show irregular fluctuations and random motion transverse to the direction of the flow; this pattern is referred to as turbulent flow.<sup>1,2</sup> The Reynolds number,  $Re = \rho d u / \eta$ , is a dimensionless parameter which is useful for characterizing the flow. Here  $\rho$  represents the density of the fluid,  $\eta$  its viscosity,  $u$  the mean velocity of the flow, and  $d$  the diameter of the pipe or orifice. The Reynolds number represents the ratio of inertial forces to viscous forces in the flow. The flow is laminar for  $Re < 2000$  and turbulent for  $Re > 4000$ . For  $Re$  between these two values, the flow may switch from laminar to turbulent conditions in a random fashion (transitional flow).<sup>1,2</sup> These effects are readily observed in the smoke from a cigarette. For the first few centimeters the smoke pattern is usually laminar. After that, the flow breaks into turbulence. In Fig. 6, we plot the value of the Reynolds number at the orifice, versus  $h$ . We see that  $Re$  varies between 4000 and nearly 400, indicating that the flow regime includes the beginning of turbulent flow, transitional flow, and laminar flow. Because our model can reproduce the experimental data using the same values of  $k$ ,  $\Delta Z$ , and  $C_v$  in all these regions of  $Re$ , the type of losses in our model and the expanded Bernoulli's equation are valid for these flow regimes. It also follows from this analysis that  $k$ ,  $\Delta Z$  and  $C_v$ , are independent of  $Re$  for the flows studied here.



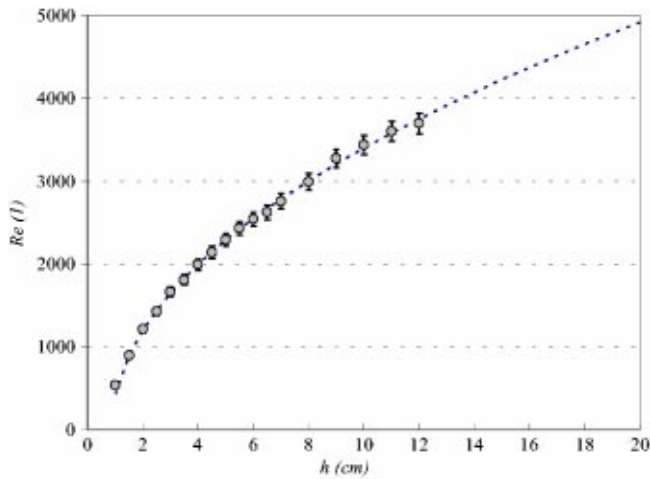


Fig. 6. The circles indicate the values of the Reynolds number at the orifice for the different values of  $h$  used in our experiment.

## V. CONCLUSIONS

The proposed experiment is simple and inexpensive, is accessible to beginning students, and illustrates the importance and usefulness of Bernoulli's equation for real fluids including energy losses, over a wide range of Reynolds numbers. All that is needed to further explore the turbulent regime is a taller cylinder. The experiment also verifies that liquid particles follow the same trajectory as solid particles, indicating that they obey the same physical laws.

The proposed model, based on the extended Bernoulli's equation, is adequate to describe qualitatively and quantitatively the physics of drainage of a vessel. Furthermore, the fitting of the theoretical model to the data allows us to extract the relevant parameters of the model, namely the coefficients  $\Delta Z$  and  $k$  of Eq. (4) and the coefficient of vena contracta  $C_v$ . The motion of the free surface is well reproduced by the model, in particular its time dependence. Furthermore, we can measure the coefficient of vena contracta in the exit jet and the coefficient of losses in our system.

## ACKNOWLEDGMENTS

We acknowledge the valuable comments and suggestions made by Professors E. Calzetta, G. García Bermúdez, C. Waltham, F. Minotti, and Dr. A. Schwint.

## APPENDIX

When a laminar flow enters into a pipe, it does not immediately develop the parabolic velocity profile that prevails

well inside the pipe. There is a transition region or entrance length,<sup>1,3</sup>  $L_e$ , over which the velocity profile changes from a planar to the fully developed parabolic profile. A semiempirical relation that allows us to estimate this entrance length is given by<sup>12</sup>

$$L_e = C_e Re d, \quad (\text{A1})$$

where  $C_e$  is a constant. Several authors have proposed different values for this constant,<sup>1,3,12</sup> but all range between 0.029 and 0.06 for laminar flows. If we applied Eq. (A1) to the exit orifice, we obtained values of  $L_e$  which were much larger than the wall thickness in all the cases we studied. Therefore, the velocity profile of the exit jet can be regarded as planar, that is,  $\alpha_2 \approx 1$ . On the other hand, for the cylinder, the average velocity is so small ( $u_1 \approx 10^{-2}$  cm/s), that  $\alpha_1 \approx 2$ .

<sup>a)</sup>Electronic mail: msaleta@labs.df.uba.ar

<sup>b)</sup>Electronic mail: dina@labs.df.uba.ar

<sup>c)</sup>Electronic mail: sgil@df.uba.ar

<sup>1</sup>B. R. Munson, D. F. Young, and T. H. Okiishi, *Fundamentals of Fluid Mechanics* (Wiley, New York, 1994), 2nd ed., Chaps. 3 and 8.

<sup>2</sup>V. L. Streeter and E. D. Wylie, *Fluid Mechanics* (McGraw-Hill, New York, 1985), 8th ed., Chap. 8.

<sup>3</sup>B. Nekrasov, *Hydraulics for Aeronautical Engineers*, translated from the Russian by V. Talmy (Mir, Moscow, 1969), Chaps. 6 and 9.

<sup>4</sup>C. E. Synolakis and H. S. Badeer, "On combining the Bernoulli and Poiseuille equation—A plea to authors of college physics texts," *Am. J. Phys.* **57**, 1013–1019 (1989).

<sup>5</sup>C. Waltham, S. Bendall, and A. Kotlicki, "Bernoulli levitation," *Am. J. Phys.* **71**, 176–179 (2003).

<sup>6</sup>J. N. Libii, "Mechanics of the slow draining of a large tank under gravity," *Am. J. Phys.* **71**, 1204–1207 (2003).

<sup>7</sup>M. Nelkin, "Resource Letter TF-1: Turbulence in fluids," *Am. J. Phys.* **68**, 310–318 (2000).

<sup>8</sup>G. T. Hageseth, "Surface and kinetic energy densities: A fluid dynamics laboratory exercise," *Am. J. Phys.* **54**, 1011–1014 (1986).

<sup>9</sup>Examples of Excel files illustrating this procedure can be downloaded from (www.fisicareCreativa.com). This site also describes experimental projects using new technologies and reports of experiments performed by undergraduate students from Latin American universities.

<sup>10</sup>B. Tolar, "The water drop parabola," *Phys. Teach.* **18**, 371–372 (1980).

<sup>11</sup>R. P. Feynman, R. B. Leighton, and M. Sands, *The Feynman Lectures on Physics* (Addison-Wesley, Reading, MA, 1964), Vol. II, Chap. 41.

<sup>12</sup>S. G. Kandlikar and L. A. Campbell, "Effect of entrance condition on frictional losses and transition to turbulence," Proceedings of IMECE2002, 17–22 November, 2002, New Orleans. IMECE2002-34573. Available at (http://www.rit.edu/~taleme/papers/conference%20papers/C058.pdf).